micro

MDPI

Article

Polyaniline Hybrids with Biological Tissue, and Biological Polymers as Physiological—Electroactive Materials

Mai Ichikawa, Masashi Otaki and Hiromasa Goto *

Department of Materials Science, Faculty of Pure and Applied Sciences, University of Tsukuba, Tsukuba 305-8573, Ibaraki, Japan
* Correspondence: gotoh@ims.tsukuba.ac.jp

Abstract: A sprout/polyaniline was synthesized via the chemical oxidative polymerization of aniline in the presence of natural sprout, based on a concept of cyborg plant composite. The composite consisted of both polyaniline and plants. The chemical structure was confirmed by infrared absorption spectroscopy measurements. Optical microscopy observation revealed that polyaniline was deposited into the micro-tissue of the sprout to form the conductive polymer bio-composite. Micro-optical fiber functions for the composite were visually confirmed. Furthermore, the sprout/polyaniline based organic diode exhibited an avalanche breakdown phenomenon. Next, a fucoidan/polyaniline composite as a physiological active material/conducting polymer composite was prepared. This composite showed good film-forming ability, electrochromism, and a micro-porous surface. This paper reports the preparation of conducting polymer composites with a combination of bio-tissue and bio-substance for the creation of bio-based electrically active organized architecture.

Keywords: avalanche diode; conductive polymer; fucoidan; polyaniline; sprout

check for updates

Citation: Ichikawa, M.; Otaki, M.; Goto, H. Polyaniline Hybrids with Biological Tissue, and Biological Polymers as Physiological—Electroactive Materials. *Micro* **2023**, *3*, 172–191. https://doi.org/10.3390/micro3010013

Academic Editor: Ajit Roy

Received: 3 January 2023
Revised: 20 January 2023
Accepted: 25 January 2023
Published: 1 February 2023

Copyright: © 2023 by the authors. Licensee MDPI, Basel, Switzerland. This article is an open access article distributed under the terms and conditions of the Creative Commons Attribution (CC BY) license (https://creativecommons.org/licenses/by/4.0/).

1. Introduction

Organic materials have been considered insulators because they have no charge carriers for electrical conduction. However, in the early 1970s, Shirakawa et al. reported the synthesis of polyacetylene as the first electrically conducting polymer [1]. Currently, conductive polymers are known as "synthetic metals" because they exhibit metallic reflection colors due to plasma reflection through free electron movement.

Based on such electrical conduction systems and light reflection, researchers are focusing on applications such as organic solar cells [2], organic light-emitting devices [3–5], and organic transistors [6–8]. However, the conjugated polymers comprising rigid structures have extremely low processability due to infusibility and insolubility. Furthermore, these polymers are unstable in the ambient atmosphere because they are sensitive to oxygen and water. Conversely, polyaniline (PANI), a conductive polymer, can be synthesized in water and is stable in air and water. However, PANI has poor processability, which limits its practical applications. To improve this drawback, introduction of flexible alkyl chains into polymers has been performed. Recently, post-modification of conductive polymers has been developed [9]. Composite formation of PANI with other polymers such as polystyrene is a solution for processing conducting polymers [10–16]. Composites based on carboxymethyl cellulose cryogel/conductive polymers have been developed [17]. Polymer/fullerene nanocomposites were synthesized for anticorrosion applications in the biomedical field [18]. Polylactic acid/PANI nanofibers were developed for applications in nerve tissue engineering [19]. Fiber-type transistors have been developed using fiber conductive polymers [20] and composite sheets [21]. The conducting composite polymer sheets can shield electromagnetic waves and remove static electricity via wiping.

A combination of synthetic polymers and biomaterials is being developed as a new category of biosynthetic cyborg materials [22–29]. Biomaterials have exquisite functions and

microstructures that are difficult to artificially process. The microstructure of biomaterials can be applied to synthesize polymers with highly ordered structures. Orientation of the primary chain is attained through the deposition of PANI along the linearly shaped plant vessels to draw high performance [30,31].

In this study, PANI is synthesized on the vessels in the vascular bundle of a plant. PANI can be well deposited on the surface of the vessels. We use sprout as a plant template for the polymer. The PANI component grows in the macroscopic helical structure of the plant vessel during polymerization. The hybrids produced in this way function as wave guides that allow the red laser to penetrate along the filamentous microstructure. Furthermore, the organic avalanche diode function of the sprout/PANI was found with combination of electrical conduction of PANI and ionic conduction.

In addition, to prepare PANI hybrids with biological tissue, we also made composites with fucoidan from sea weed. Fucoidan is a polysaccharide consisting of a six-ring structure, plural stereogenic centers, and glycoside bonding, and has been paid attention for its functions [32] such as antithrombotic [33], anti-tumor [34], anti-virus [35], anti-allergic activities [36,37]. The application of fucoidan as a marine fiber has potential for new technological developments [38–47]. Fucoidan is obtained from sea weeds. Fucoidan mainly consists of three types of structure, U-fucoidan, G-fucoidan, and F-fucoidan, as shown in Figure 1. We discovered that fucoidan gel can be conveniently prepared by two steps: (1) addition of NaOH to the water, and (2) subsequent addition of sulfuric acid. The gel can be used as both a reaction field and a component for the construction of a fucoidan/polyaniline composite, abbreviated as fucoidan/PANI. In this study, oxidative polymerization of aniline in the dispersion of non-gel fucoidan in the water, chemical polymerization in the fucoidan gel, and electrochemical polymerization in the fucoidan gel are carried out. The fucoidan/PANI composite thus prepared shows a good redox property, which is confirmed by cyclic voltammetry. The composite exhibits electrochromism during the redox process. The surface color is changed from green to dark blue during the electrochemical oxidation (doping) preprocess. X-ray diffraction (XRD) measurements revealed that the fucoidan as a reaction field provides a higher order structure for the resultant. The surface structure of the fucoidan/PANI exhibited high porous structure. Increasing the fucoidan content in the fucoidan/PANI composite increases the fine fraction size of the composite.

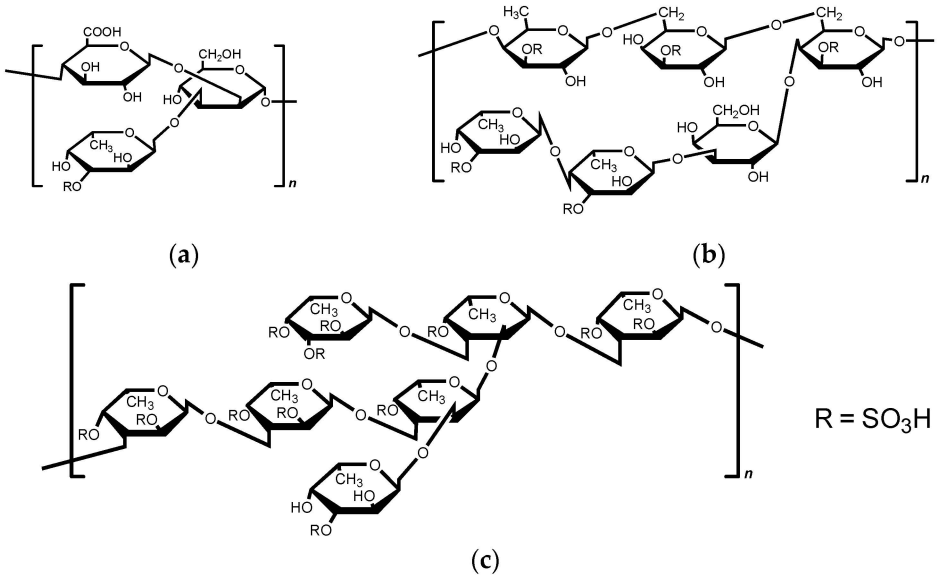

Figure 1. Chemical structures of fucoidans. (**a**) G-fucoidan, (**b**) U-fucoidan, (**c**) F-fucoidan.

PANI hybrids have attracted much attention for their applications [48,49]. The combination of PANI with bio-tissues and bio-chemical materials represents a new approach to the development of organic functional conductive materials.

2. Materials and Methods

2.1. Materials

Aniline monomer (Nacalai Tesque, Inc., Kyoto, Japan), sulfuric acid (Nacalai Tesque, Inc., Kyoto, Japan), ammonium persulfate (APS, Yoneyama Yakuhin Kogyo Co., Ltd., Osaka, Japan), *N*-methylpyrrolidone (NMP, Tokyo Chemical Industry Co., Ltd., Tokyo, Japan), and crude fucoidan (*Kjellmaniella crassifolia* (kelp)), code no. 4490, consisting of fucose 37.3%, uronic acid 5.48%, sulfur 5.48%, ash 28.1%, and H_2O 1.86% (TAKARA BIO Inc., Kusatsu, Japan), were used as obtained. Sprouts were purchased from Narita Foods (Soma City, Japan).

2.2. Measurements

Fourier Transform Infrared (FT-IR) absorption spectroscopy measurements were performed via the KBr method in a 400–4000 cm^{-1} range using FT-IR 4600 equipment (JASCO, Tokyo, Japan). Optical observations were conducted using a high-resolution polarizing microscope (ECLIPS LV 100, Nikon) with an LU Plan Fluor lens and CFIUW lens (Nikon, Tokyo, Japan). Ultra-violet visible (UV-vis) spectra were recorded on a JASCO V-630 spectrophotometer (JASCO, Tokyo, Japan). Electron spin resonance (ESR) measurements were carried out using a JEOL JES TE-200 spectrometer with 100 kHz modulation, X-band (JEOL, Tokyo, Japan). Scanning electron microscopy (SEM) observations were performed with a JEOL JSM-521 (JEOL, Tokyo, Japan). Cyclic voltammetry was carried out with a μAUTOLAB TYPE III (ECO Chemie, the Netherlands). The X-ray diffraction (XRD) measurements were carried out with a RINT2100 (Rigaku, Tokyo, Japan).

2.3. Synthesis of Sprout/PANI

Aniline monomer (2 g) and sulfuric acid (3 g) in water (200 mL) were cooled with an ice bath. Subsequently, sprouts (1.3 g) were dispersed in the water, and ammonium persulfate (2 g) as a polymerization initiator was added. After 24 h, the crude composite was filtered and washed with a large volume of methanol and water. The product was filtered, collected, and dried naturally to yield 0.11 g of sprout/PANI composite. The synthetic formula for the preparation of this hybrid material is displayed in Scheme 1.

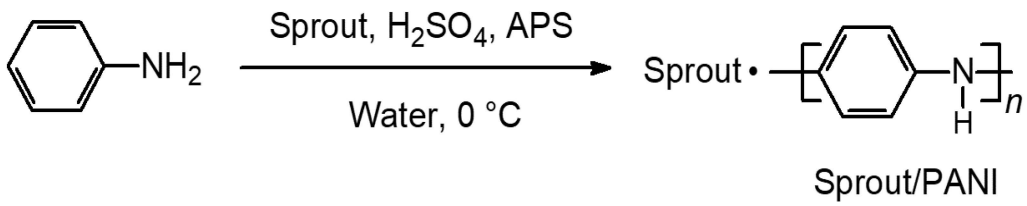

Scheme 1. Synthesis of sprout/polyaniline (sprout/PANI) composite. APS: ammonium persulfate.

2.4. Synthesis of PANI with Fucoidan

2.4.1. Synthesis of Polyaniline with Non-Gel Method

Polymerization of aniline in the presence of fucoidan to yield fucoidan/PANI composites was carried out. Fucoidan with no treatment with NaOH has low solubility in water, causing a form of fucoidan particles to remain as precipitate in the water. Preparation of a PANI composite with non-gel fucoidan as a form of microparticles is denoted as the non-gel method. The products are abbreviated as N05-5. Table 1 summarized synthesis and results for the fucoidan/PANI with the non-gel method. Increasing the amount of fucoidan in the polymerization decreased the resultant quantity.

Table 1. Non-gel polymerization of aniline in the presence of fucoidan with oxidative chemical polymerization.

	Fucoidan (g)	Product (g)
Fucoidan/N05	0.05	Powder (0.120)
Fucoidan/N1	0.1	Powder (0.183)
Fucoidan/N2	0.2	Powder (0.199)
Fucoidan/N3	0.3	Powder (0.180)
Fucoidan/N4	0.4	Powder (0.198)
Fucoidan/N5	0.5	Powder (0.029)

Monomer (aniline, 0.6 g), water (10 mL), ammonium persulfate (APS, 0.49 g), reaction time = 24 h.

Preparation of PANI in the presence of fucoidan with the non-gel method was carried out as follows. First, 0.05 g (Fucoidan/N05), 0.1 g (Fucoidan/N1), 0.2 g (Fucoidan/N2), 0.3 g (Fucoidan/N3), 0.4 g (Fucoidan/N4), or 0.5 g (Fucoidan/N5) of fucoidan were added to distilled water (50 mL) containing aniline (0.2 g) and stirred for 1 night. Then, the mixture was cooled with an ice bath. APS (0.49 g, 2.1 mmol) dissolved in 10 mL of water was slowly dropped into the mixture to initiate oxidative polymerization. The reaction was continued for 24 h. Then, the crude product was collected by filtration and washed with a large volume of distilled water and methanol until the filtrate was colorless. Subsequent vacuum drying yielded the desired product (Scheme 2).

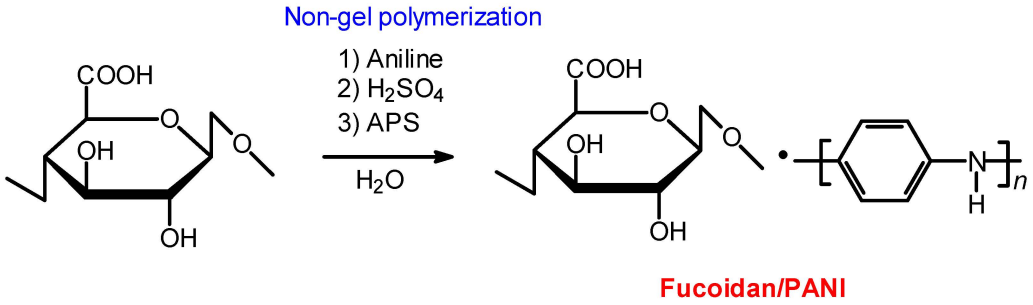

Scheme 2. Synthesis of fucoidan/polyaniline (fucoidan/PANI). Polymerization of aniline in the presence of fucoidan with non-gel polymerization. APS, ammonium persulfate; PANI, polyaniline.

2.4.2. Synthesis of Polyaniline with Chemical Reaction in Fucoidan Gel

Fucoidan dissolved well in the NaOH/water solution because the OH and COOH group were changed to anions (–O^-·Na^+, –COO^-·Na^+), as shown in Scheme 3. First, aniline was dissolved in the fucoidan salt/water solution. Addition of sulfuric acid changes the solution to the gel form due to protonation of fucoidan. In this time, the fucoidan gel as a matrix contained aniline monomer. Polymerization of aniline as a monomer allowed it to grow well in the fucoidan gel reaction field. PANI prepared with the fucoidan gel method yielded a deep green powder in the form of emeraldine salt. Polymerization and the results of it are summarized in Table 2. Here, pure PANI prepared by chemical oxidative polymerization is denoted by C-PANI, the fucoidan/PANI composite prepared in the fucoidan gel by the chemically oxidative polymerization is denoted by fucoidan/C-PANI (gel), pure PANI prepared by electrochemical polymerization is denoted by E-PANI, and the fucoidan/PANI composite prepared in the fucoidan gel by electrochemical polymerization is denoted by fucoidan/E-PANI (gel).

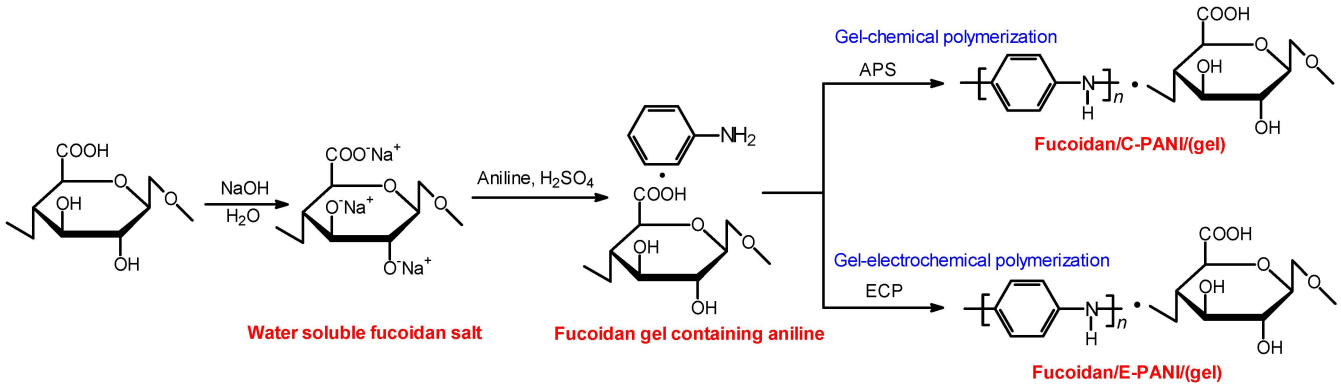

Scheme 3. Gel-chemical polymerization and gel-electrochemical polymerization. ECP, electrochemical polymerization.

Table 2. Polymerization of aniline in the presence of fucoidan with oxidative chemical polymerization and electrochemical polymerization [a]. C-PANI, pure PANI prepared by chemical oxidative polymerization; fucoidan/C-PANI(gel), a composite prepared in the gel by chemical oxidative polymerization; E-PANI, pure PANI prepared by electrochemical polymerization; fucoidan/E-PANI(gel), a fucoidan/PANI composite prepared in the fucoidan gel by electrochemical polymerization.

	Fucoidan (g)	APS (g) [b]	*E* (V) [c]	*T* [d]	Product
C-PANI	-	0.6	-	24 h	Powder (0.214 g)
Fucoidan/C-PANI(gel)	0.5	0.6	-	24 h	Powder (0.525 g)
E-PANI	-	-	4.0	10 min	Film
Fucoidan/E-PANI(gel)	0.5	-	4.0	10 min	Film

[a] Monomer (aniline, 0.6 g), water (10 mL), [b] ammonium persulfate, [c] application voltage, and [d] reaction time.

Preparation of fucoidan/C-PANI(gel) with chemical polymerization was carried out as follows (Scheme 3). First, aniline (0.6 g, 6.44 mmol), fucoidan (0.5 g) and a small amount of sodium hydroxide (NaOH) were added to distilled water (10 mL) and stirred for 30 min. After confirmation that the fucoidan was completely dissolved in the aqueous solution, it was cooled with an ice bath, and sulfuric acid (0.6 g, 6.12 mmol) was added to the mixture. The solution appeared to have high viscosity; however, the stirring was continued. Ammonium persulfate (APS, 0.6 g, 2.63 mmol) dissolved in a small amount of water was slowly dropped into the mixture to initiate oxidative polymerization. The stirring was continued for 24 h. Then, the crude product was collected by filtration and washed with a large volume of distilled water and methanol until the filtrate was colorless. Subsequent vacuum drying yielded a dark green powder as a desired product (0.525 g).

2.4.3. Synthesis of Polyaniline with Electrochemical Reaction in Fucoidan Gel

Preparation of PANI with electrochemical polymerization was carried out as follows (Scheme 3). Aniline (0.6 g, 6.44 mmol), fucoidan (0.5 g) and small amount of sodium hydroxide (NaOH) were added to distilled water (10 mL) and stirred for 30 min. Then, the mixture was cooled with an ice bath, and sulfuric acid (0.6 g, 6.12 mmol) was added to the mixture. Then, electrochemical polymerization was carried out by a two-electrode system using indium tin oxide (ITO)-coated glass for the anode and cathode. A potential of DC 4.0 V was applied across the cell, and the polymerization reaction was carried out for 10 min. Vacuum drying then yielded a dark green film deposited on the ITO (anode side). This method can be referred to as "gel-electrochemical polymerization".

3. Results and Discussion

3.1. Sprout/PANI

3.1.1. Fourier Transform Infrared (FT-IR) Spectroscopy

Figure 2 depicts the FT-IR absorption spectroscopy measurement results of the pure sprout and the sprout/PANI composite. Figure 3 displays the chemical structure of cellulose for reference. The characteristic peaks of PANI, including the stretching vibration of C–H in the aromatic ring (2937 cm^{-1}), the stretching vibration of two N atoms adjacent to the quinoid ring (1613 cm^{-1}), the stretching vibration of two N atoms adjacent to the benzene ring (1495 cm^{-1}), the in-plane bending vibration of C–H in the aromatic ring (1167 cm^{-1}), and the out-of-plane bending vibration of C−H in the aromatic ring (768 cm^{-1}), were observed in the FT-IR absorption spectra of the sprout/PANI (Figure 2a). The O–H and C–O–C stretching vibrations (at 3410 cm^{-1} and 1039 cm^{-1}, respectively) originated from cellulose, which is the main component of a plant cell or plant fiber. Three absorption bands between 1300 and 1700 cm^{-1} were indicative of the amide bonds such as amide I, II, and III (Figure 2b), which were originated from the soy protein of sprout. The sprout has both proteins and cellulose components. The chemical structure of cellulose is displayed in Figure 3 as a reference. The vibrational modes of the amide group are indicated in Figure 4. Therefore, the FT-IR spectra confirmed that the composites consist of polyaniline and sprout.

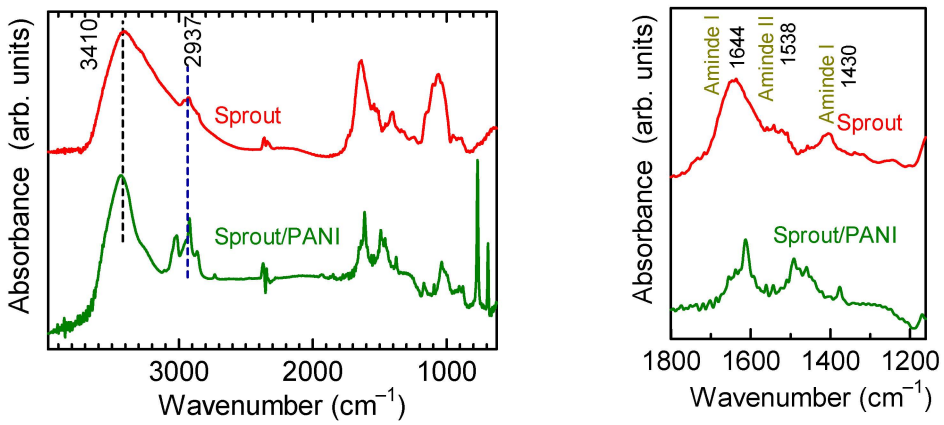

Figure 2. (**a**) Fourier transform infrared (FT-IR) absorption spectra of the pure sprout and sprout/polyaniline (sprout/PANI). (**b**) Magnification of the FT-IR absorption spectra of the sprout and sprout/PANI.

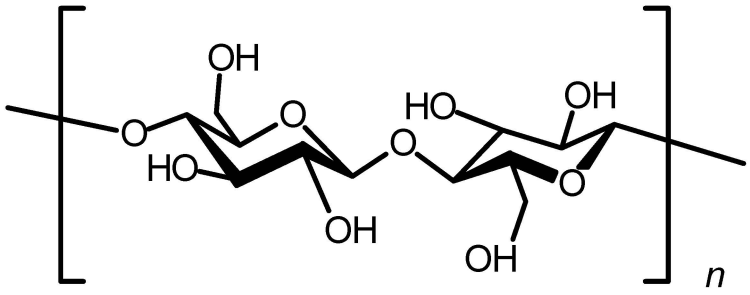

Figure 3. Chemical structure of cellulose.

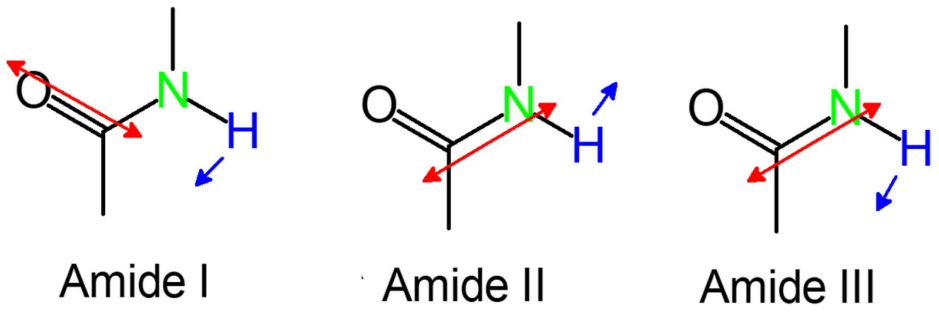

Figure 4. Vibrational modes of amide I, amide II, and amide III. Red arrows, C=O and N–H stretching; Blue arrows, N-H vending.

3.1.2. Optical Microscopy Images

Figure 5a displays an optical microscopy image of the sprout plant cells. Inside the cell wall, a helical structure was observed (Figure 5b). This helix, a secondary cell wall, winds on the vessel of sprout (Figure 6). The helical structure of the vessel was clearly observed in the optical microscopy images of sprout/PANI (Figure 7a,b). The emerald color of the images was caused by polyaniline in the composite. PANI was located inside the vessel because the vessel in water contained an aniline monomer which was polymerized during the polymerization reaction to form wire-formed PANI in the vessel. The plausible deposition of the wire-formed PANI component is depicted in Figure 8.

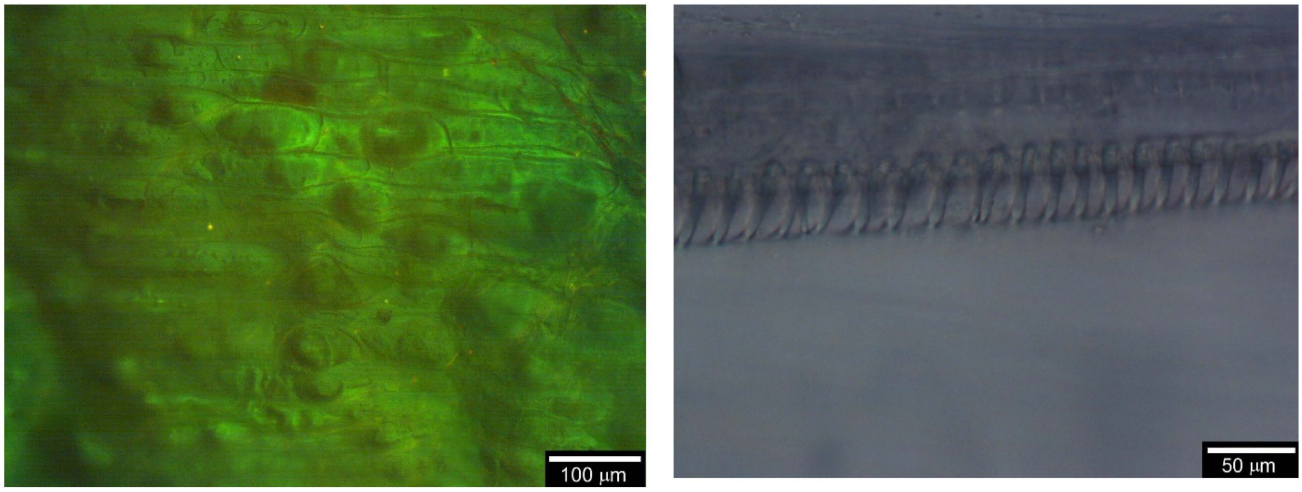

(**a**) (**b**)

Figure 5. Optical microscopy images of sprout (**a**) the plant cells of sprout, (**b**) inside the cell wall, showing a helical structure.

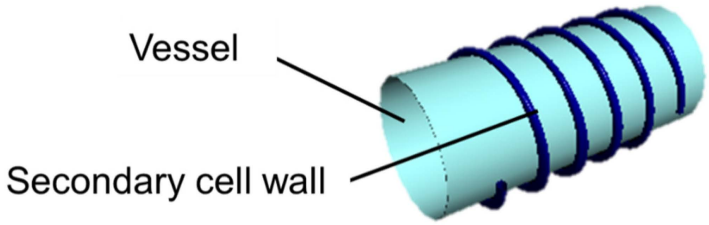

Figure 6. Structure of a vessel.

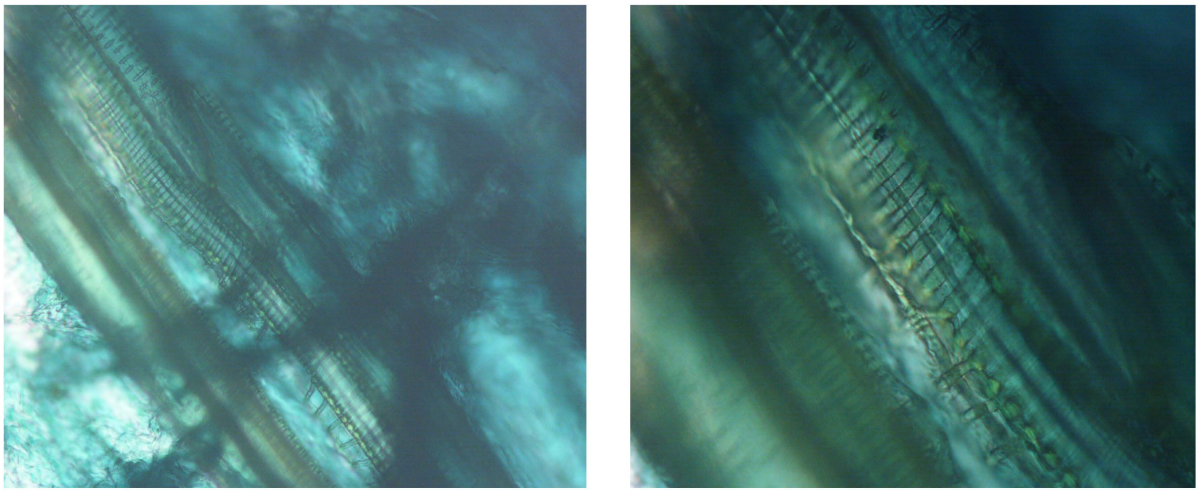

(**a**) (**b**)

Figure 7. Optical microscopy images of sprout/PANI at low magnification (**a**) and high magnification (**b**).

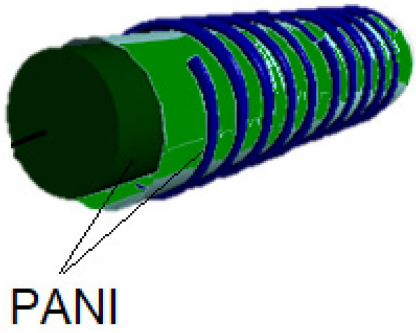

Figure 8. Three-dimensional image of the sprout with PANI wire.

Laser irradiation of sprout/PANI showed light conduction along the sprout/PANI composite vessel fiber. Figure 9a,b show optical microscopy images of sprout/PANI without laser irradiation and with laser irradiation, respectively. The plausible light conduction depicted in Figure 10 indicates that the composite is a natural textile and the conducting polymer composite strings have a fine optical fiber function.

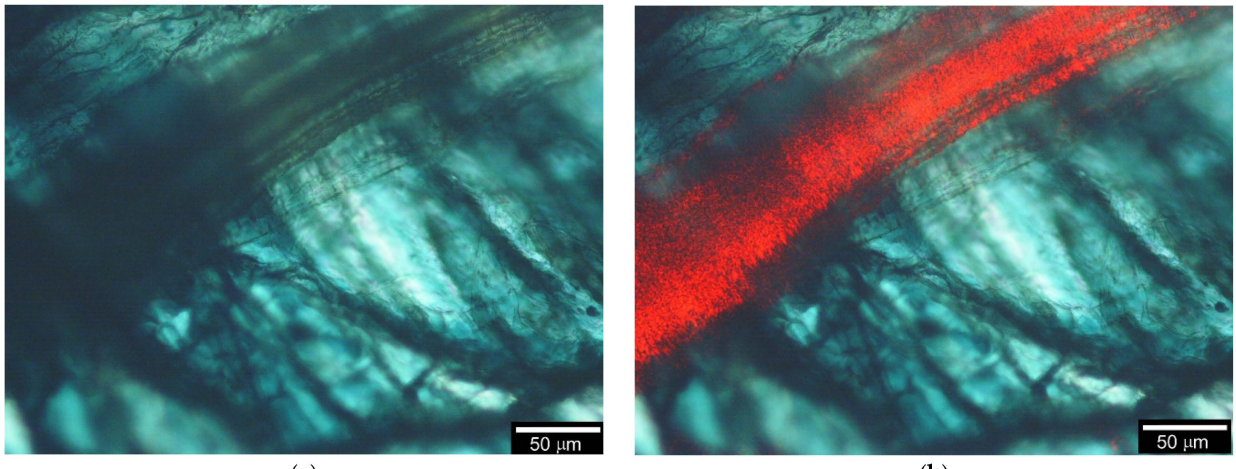

(**a**) (**b**)

Figure 9. Light conduction function of sprout/PANI composite under (**a**) no light irradiation, and (**b**) light conduction along the sprout/PANI vessel composite upon red laser light irradiation.

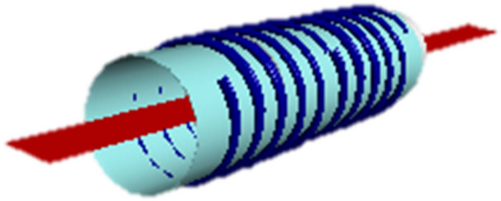

Figure 10. Three-dimensional image of sprout/PANI.

3.2. Fucoidan/PANI

3.2.1. IR Absorption

Figure 11 displays the IR spectra of fucoidan, C-PANI (pure PANI) as a reference, fucoidan/N5 prepared by the non-gel method, and fucoidan/PANI(gel), showing characteristic bands at 3502 cm^{-1} and 1647 cm^{-1} due to a hydroxyl group and carboxyl group. The absorption band at 1570 cm^{-1} is due to the C=C stretching vibration of quinonoid (Q), and at 1481 cm^{-1} is due to a benzenoid (B) structure, as shown in Figure 11 (top). The absorption bands at 1300 cm^{-1} and 1248 cm^{-1} are due to the C–N stretching absorption of QBQ and BBB structures, respectively. Absorption bands at high wavenumbers are well known as characteristic bands of PANI. Molecular interactions between PANI and fucoidan may suppress the IR absorptions of OH and COOH groups in the resultant materials.

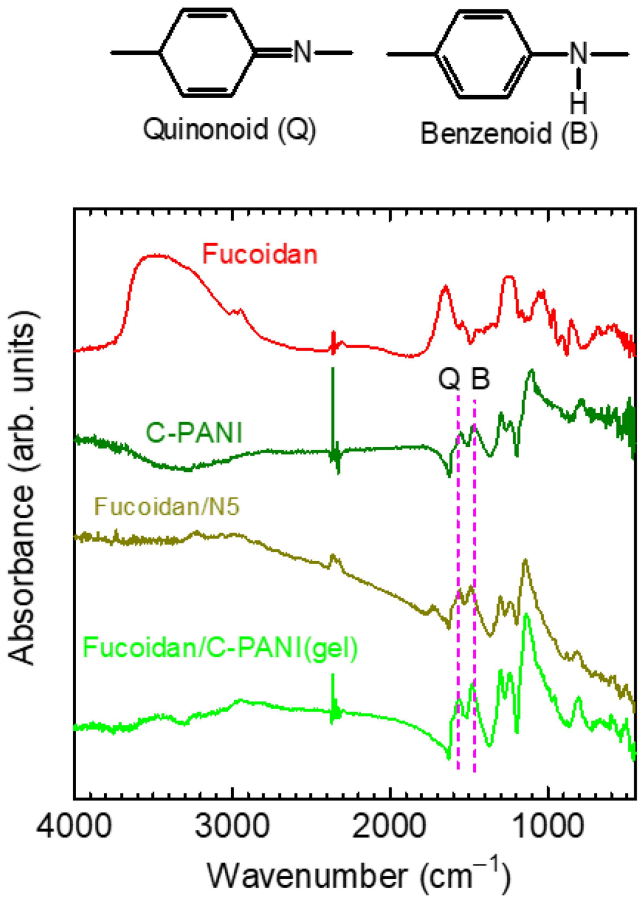

Figure 11. Fourier transform infrared (FT-IR) absorption spectra of fucoidan, C-PANI, fucoidan/N5 prepared by non-gel method, and fucoidan/C-PANI(gel).

3.2.2. UV-vis Absorption

Figure 12 shows optical absorption spectra of fucoidan, C-PANI (pure polyaniline, reference), fucoidan/E-PANI(gel), and fucoidan/C-PANI(gel). Fucoidan shows no characteristic absorption at 300–900 nm. C-PANI exhibits absorptions at 334 nm due to absorption

of the monomer repeat unit, and at 622 nm due to a doping band. The doping band is derived from radical cations in the main chain, referred to as polarons. The fucoidan/C-PANI(gel) displayed optical absorption at 597 nm. The blue shift in the absorption is due to twist in the main chain produced in the fucoidan matrix, because fucoidan forms a helical structure at the molecular level. The fucoidan/E-PANI(gel) shows an absorption band at 788 nm due to a doping band.

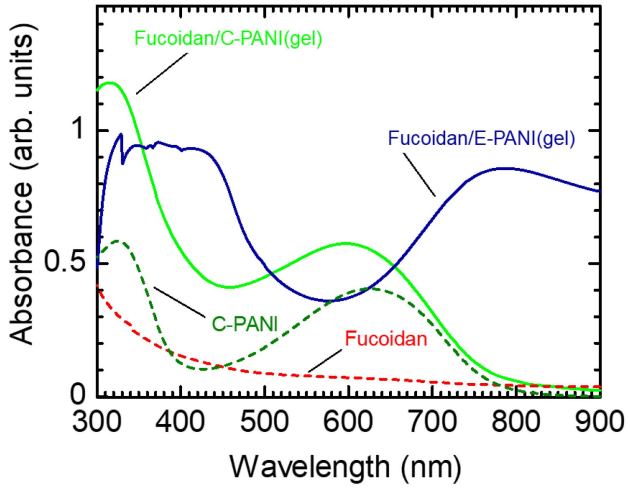

Figure 12. Optical absorption spectra of the pure fucoidan, C-PANI, fucoidan/C-PANI(gel), and fucoidan/E-PANI(gel).

3.2.3. Electron Spin Resonance

Figure 13 shows electron spin resonance (ESR) measurement results for PANI prepared with fucoidan (non-gel method, N05-5). The spin concentration (N_s) of the fucoidan/N05-5 is decreased with quantity of fucoidan in the polymerization. This may be due to the fact that increasing the fucoidan element in the composite decreases the total number of spins in the certain sample, and polymerization activity is decreased when the fucoidan element is increased in the case of polymerization with the non-gel method. The ESR peak-to-peak line width (ΔH_{pp}) increases with an increase in the fucoidan element in the polymerization. An increase in the ΔH_{pp} value indicates progress in spin localization in the main chain due to depression of charge mobility.

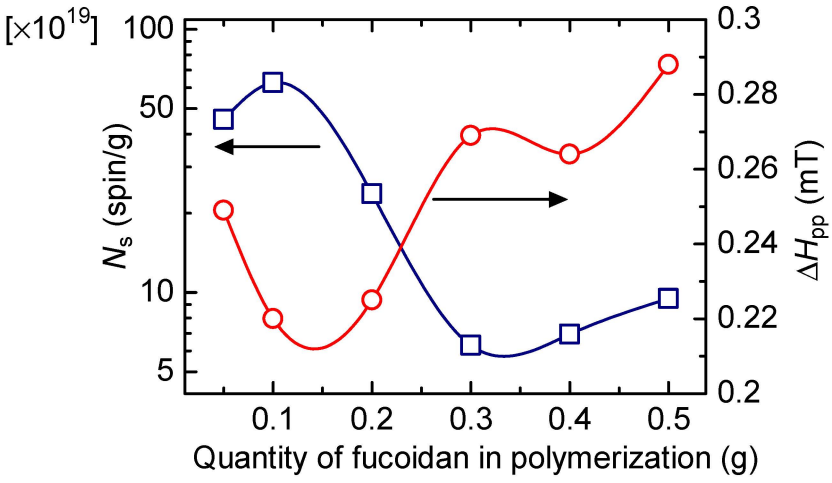

Figure 13. Electron spin resonance (ESR) results for PANI prepared with fucoidan (non-gel method, N05-5). Change in the spin concentration (N_s) (blue line) and the ESR peak-to-peak line width (ΔH_{pp}) (red line) vs. quantity of fucoidan in polymerization.

Figure 14 displays line shapes of the ESR spectra for C-PANI (pure PANI) as a reference and fucoidan/C-PANI(gel). The spectra were Lorentz-type asymmetric shape. The *g*-value of C-PANI was to be 2.00246, N_s (spin conc) 2.353 × 10^{19} spins/g, and ΔH_{pp} 0.347 mT. The fucoidan/C-PANI(gel) showed a *g*-value of 2.00266. N_s was to be 3.005 × 10^{19} spins/g, and ΔH_{pp} 0.569 mT. The fucoidan/C-PANI(gel) also exhibited broadening of the line width.

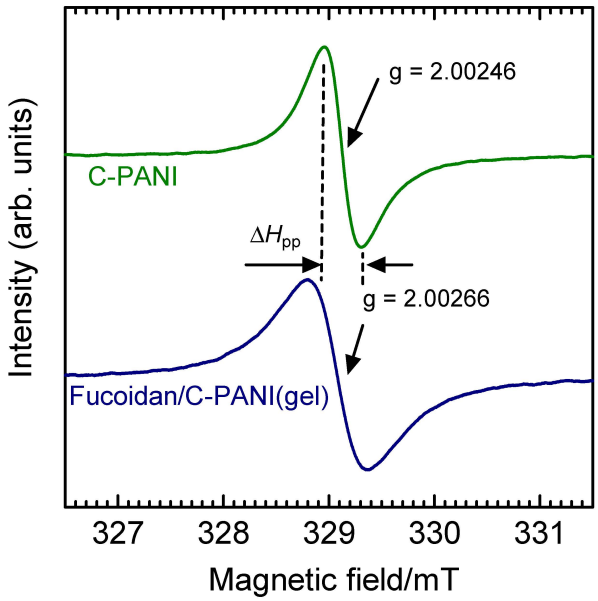

Figure 14. Electron spin resonance (ESR) line shapes of C-PANI (green line) and fucoidan/C-PANI(gel) (blue line).

3.2.4. Cyclic Voltammetry

Figure 15 shows the cyclic voltammetry (CV) measurement results of fucoidan/E-PANI(gel) deposited on the ITO glass in tetrabutylammonium perchlorate (TBAP, 0.1 M)/acetonitrile solution. Two oxidation signals of 0.38 V and 0.88 V, corresponding to electrochemical generation of polarons and bipolarons in the main chain, appeared. Further, the polymer showed two reduction signals due to bipolaron–polarons and polaron–neutral states (de-doped). This result indicates that the film is electro-active and shows a two-electron redox system in the electrochemical reaction.

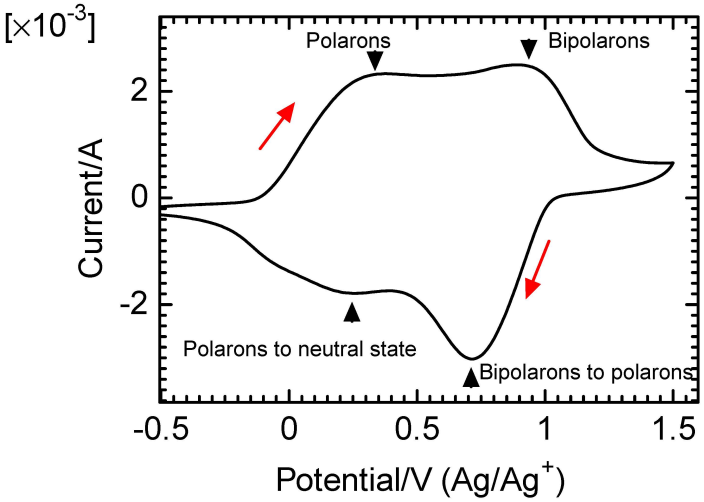

Figure 15. Cyclic voltammetry (CV) of fucoidan/E-PANI(gel) vs. Ag/Ag^+ as a reference electrode in tetrabutylammonium perchlorate (TBAP, 0.1 M)/acetonitrile solution. Arrows indicate the direction of the sweep.

3.2.5. Electrochromism

Figure 16 shows the color change of fucoidan/E-PANI(gel) by electrochemical application of voltage against an Ag/Ag^+ reference electrode in 0.1 M TBAP/acetonitrile solution. The composite changed in color from green to dark blue upon application of voltage from −0.25 V to 1.0 V. This change in color was repeatable.

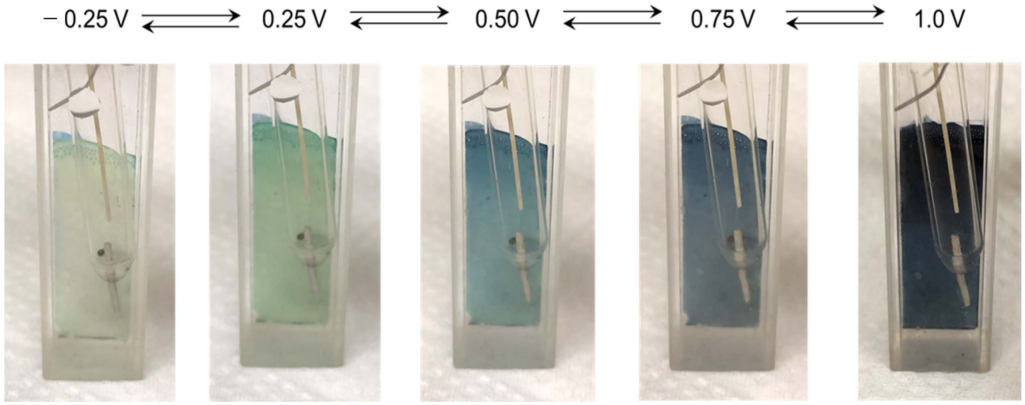

Figure 16. Change in color of electrochemically prepared fucoidan/E-PANI(gel) film deposited on indium tin oxide (ITO)-coated glass upon application of voltage between −0.25 V and 1.0 V in 0.1 M TBAP/acetonitrile solution.

3.2.6. X-ray Diffraction (XRD)

C-PANI (pure polyaniline) showed distinct diffraction signals at 15.12°, 20.60°, and 25.74° (=2θ), corresponding to *d*-spacing of 5.86, 4.31, 3.46 Å in the XRD (Figure 17). The fucoidan/C-PANI(gel) showed distinct diffraction signals at 11.98°, 15.14°, 21.06°, 25.54°, 29.62° and 31.86° (=2θ), corresponding to *d*-spacing of 7.39, 5.85, 4.22, 3.49, 3.02, 2.81 Å, respectively. Meanwhile, the pure fucoidan shows no characteristic diffraction peak in the XRD. The diffraction signals of fucoidan/C-PANI(gel) at 7.39, 3.02, and 2.81 Å indicate that the fucoidan gel produced a further ordered structure for PANI.

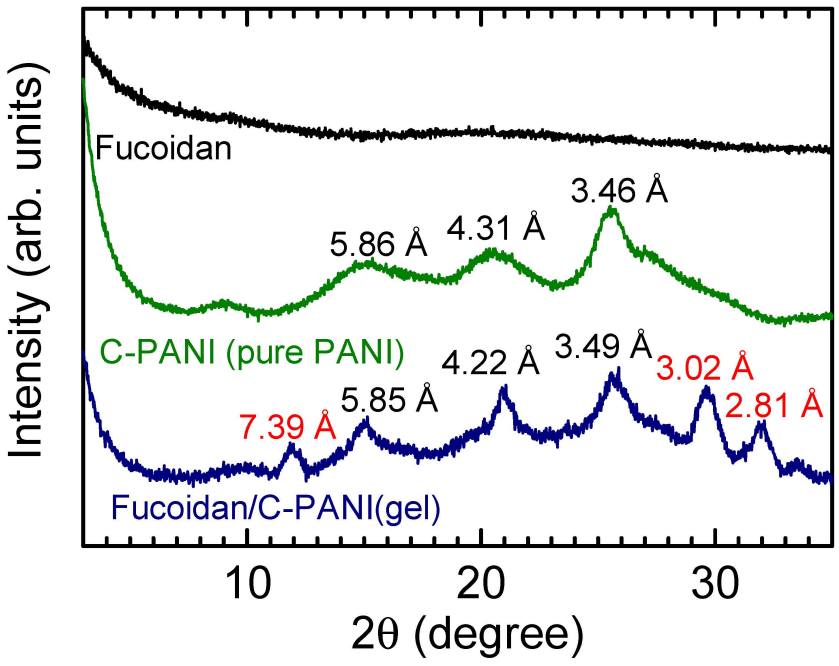

Figure 17. X-ray diffraction (XRD) profile of pure fucoidan (black line), C-PANI (pure polyaniline, green line) and fucoidan/C-PANI(gel) (blue line).

3.2.7. Surface Image

Scanning electron microscopy (SEM) and optical microscopy observations were carried out for evaluation of the surface structure. Figure 18 shows a surface image of fucoidan (Figure 18a), fucoidan/C-PANI(gel) (Figure 18b,c), and an optical microscopy image of fucoidan/E-PANI(gel), Figure 18d. The fucoidan/C-PANI(gel) exhibited a sponge-like structure, and sticks can be observed in the sample, as shown in Figure 18c. The dispersed structure of fucoidan/E-PANI(gel) was observed under optical microscopy, Figure 18d. The SEM images of N05, N1, N2 are shown in Figure 19a–f. Additionally, the SEM images of N3, N4, and N5 are shown in Figure 20a–f. The composite displayed a series of fine structures. Particularly, N5 showed a micro-domain-like structure on the surface, as shown in Figure 20e,f. Increasing the fucoidan element in the composite increased the size of the fine bulk.

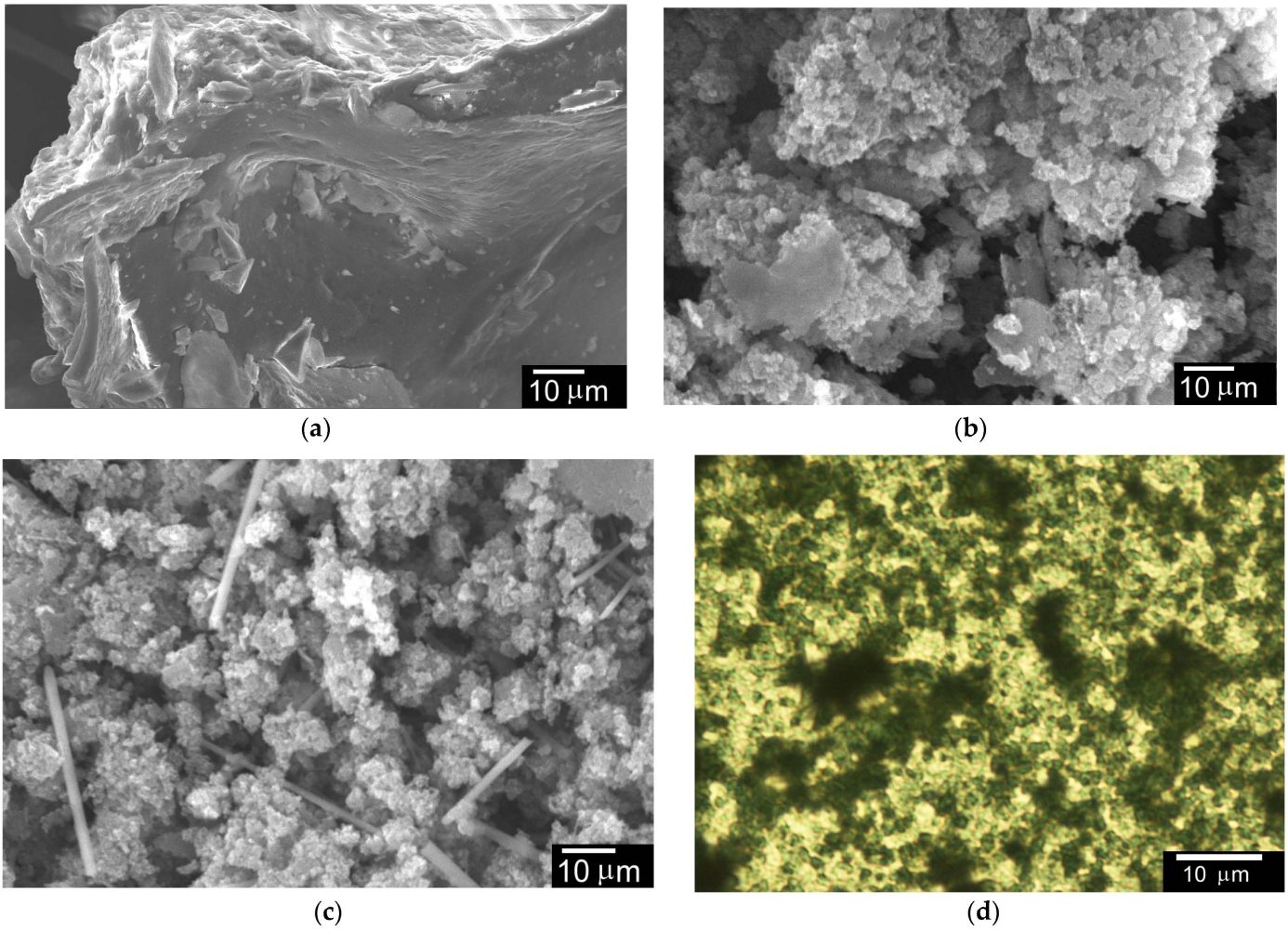

(**a**) (**b**)

(**c**) (**d**)

Figure 18. Scanning electron microscopy (SEM) and optical microscopy images of fucoidan and polymer composites. (**a**) fucoidan, (**b**,**c**) fucoidan/C-PANI(gel), and (**d**) optical microscopy image of fucoidan/E-PANI(gel).

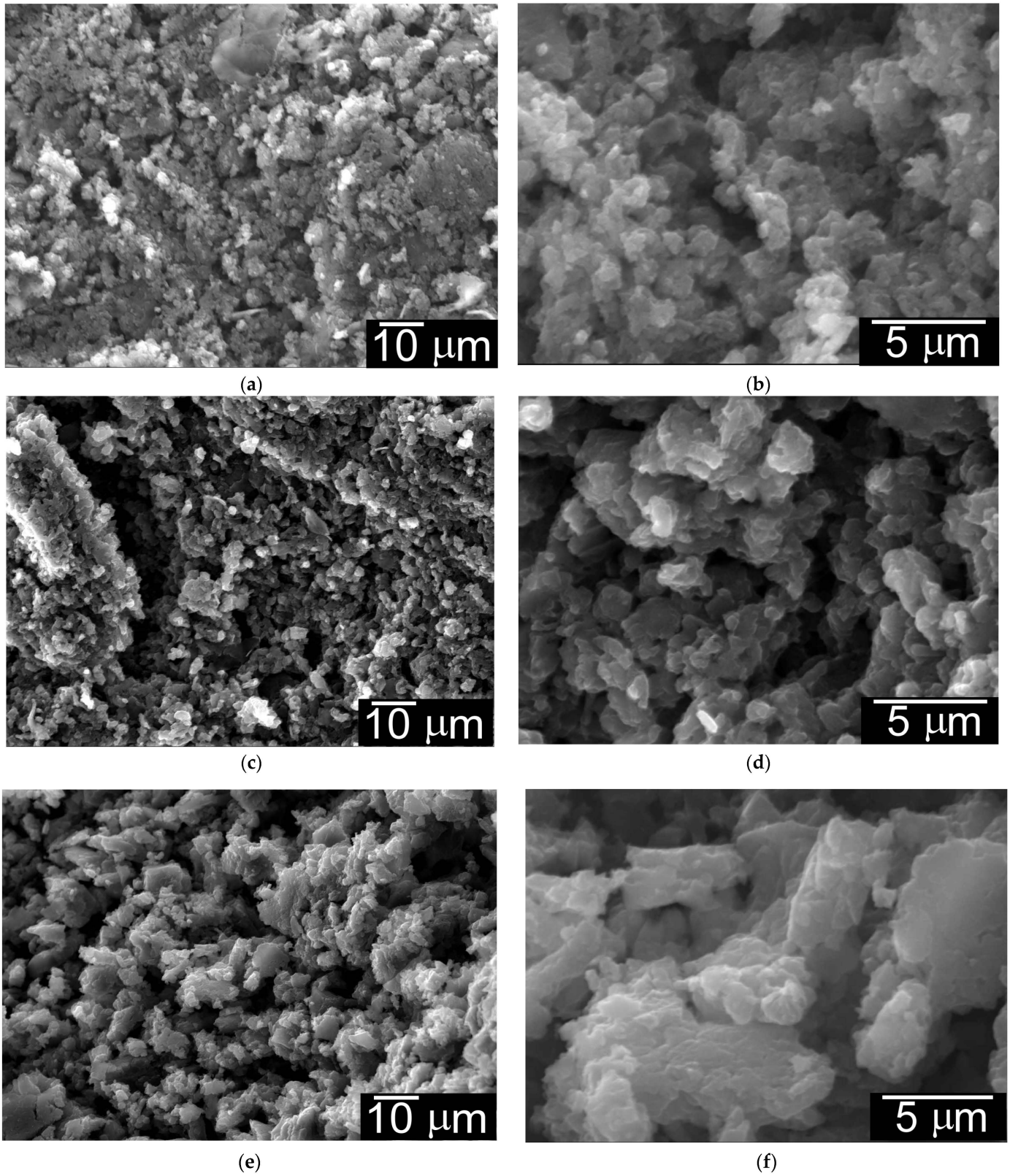

Figure 19. SEM images of polymer composites. (**a**,**b**) N05, (**c**,**d**) N1, and (**e**,**f**) N2. Increasing the of quantity of the fucoidan element in the composite increased the size of the fine bulk.

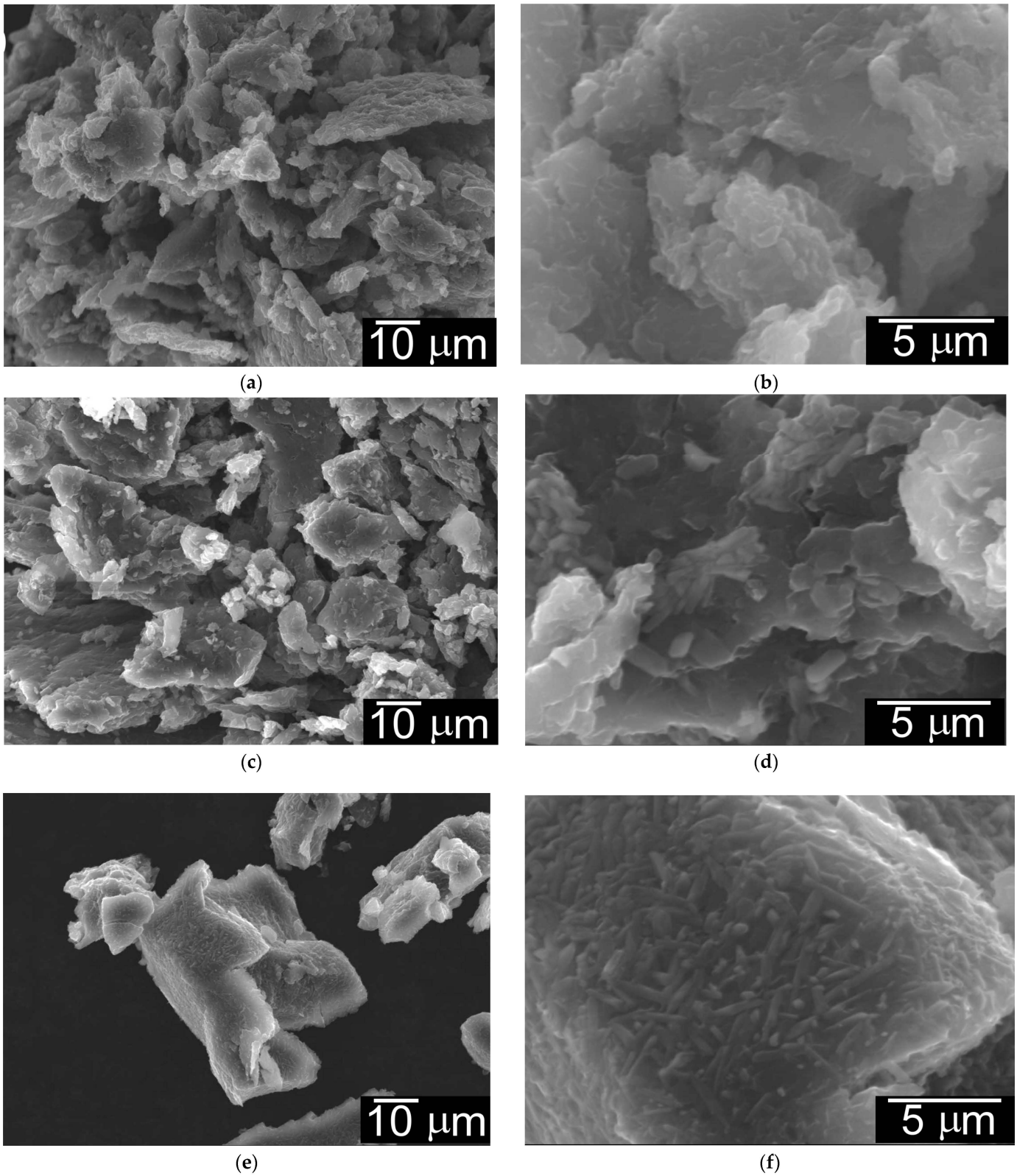

Figure 20. SEM images of polymer composites. (**a**,**b**) N3, (**c**,**d**) N4, and (**e**,**f**) N5. Increasing the fucoidan element in the composite increased the size of the fine bulk. A domain-like structure was observed on the surface of N5.

4. Diode

A diode was fabricated using sprout/PANI as an application. First, filter paper soaked in sulfuric acid, which was used as an electrolytic solution, was placed on one terminal, and gold was deposited on the opposite terminal. Subsequently, the two electric probes were connected to the terminals of the composite.

The current was measured by changing the voltage from 12 V to −12 V with gold probers (Figure 21a). The electronic symbol and sprout/PANI-based electronic circuit are depicted in Figure 21b. The current gradually decreased to 0 V from the high voltage range (electronic conduction). The insulator range showed no current flow at 0 V. However, the current flowed again at −9 V in a negative direction with ionic conduction, as shown in Figure 22.

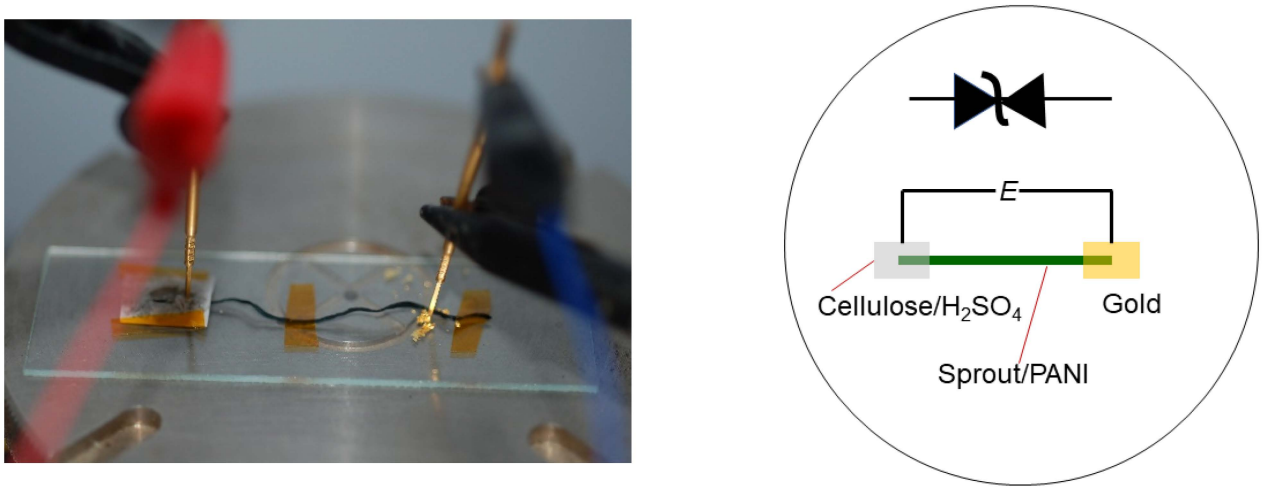

(**a**) (**b**)

Figure 21. (**a**) Setup of sprout/PANI based electrochemical diode. (**b**) Electronic symbol and circuit of the sprout/PANI electrochemical diode.

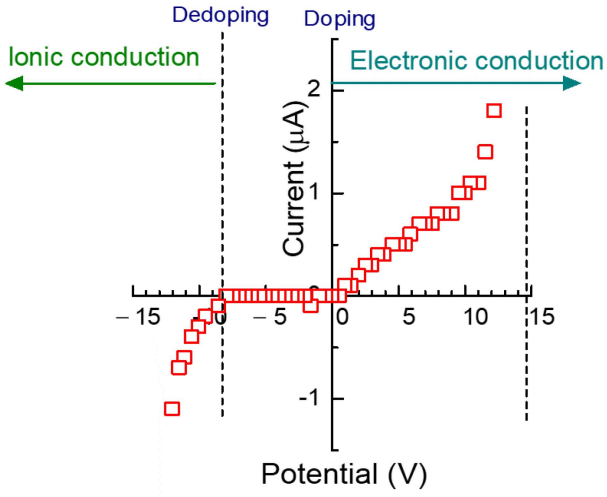

Figure 22. Current change as a function of applied voltage for the sprout/PANI electrochemical device.

Figure 23a–c show the mechanism of current change upon applying voltage to the composite device. First, PANI was electrochemically doped at >0 V range by the application of voltage, which made the PANI component a conductor (Figure 23a). Subsequently, in the range from 0 to −9 V, PANI was electrochemically de-doped by the application of reverse

voltage (Figure 23b). In this range, sprout/PANI behaved as an insulator, and no current flowed, owing to the electrochemical de-doping of the sulfuric ion. However, a current flow in the range of ≤ -9 V was caused by the ionic conduction of the sulfuric acid (Figure 23c).

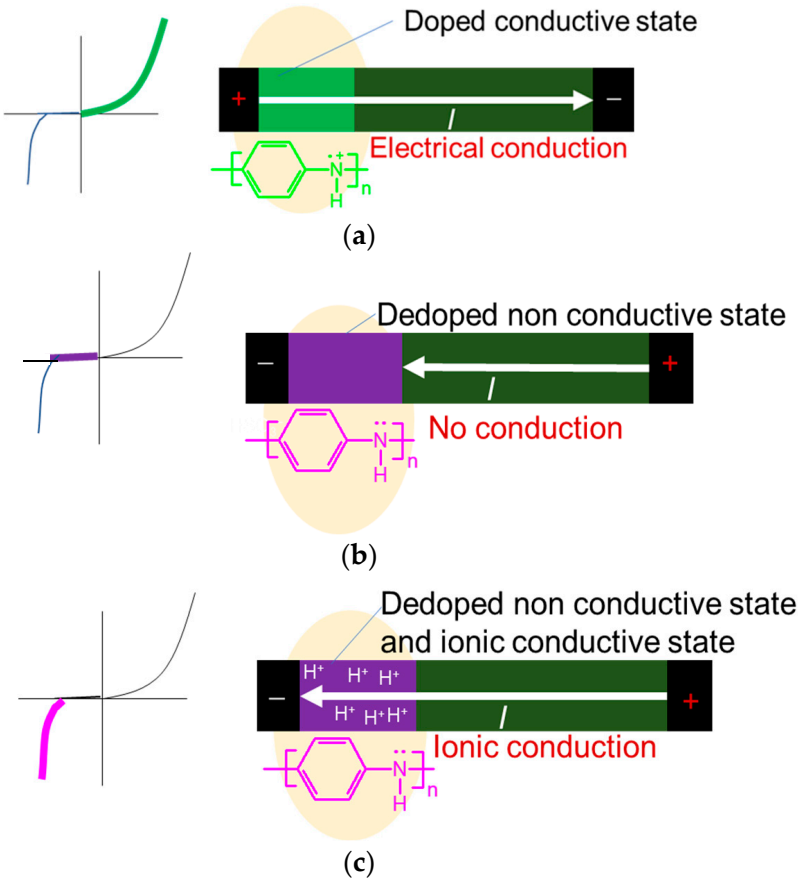

Figure 23. Mechanism of the sprout/PANI avalanche diode. (**a**) 12 to 0 V (electrical conduction state; green line), (**b**) 0 to −9 V (non-conduction state; purple line), and (**c**) −9 to −12 V (ionic conduction state; pink line).

This phenomenon is similar to the avalanche diodes of the inorganic semiconductor device experiencing an "avalanche breakdown". Although the mechanism differs from that for inorganic semiconductors, we successfully developed an avalanche-type electrochemical diode using a conductive polymer via ionic and electronic conduction. In this diode, the sprout functioned as a textile template for PANI, and the linear form of PANI was mechanically maintained in the composite.

5. Conclusions

A combination of natural plants and synthetic conducting polymers can be applied as novel organic functional devices. So far, cyborg plants with transistor functions, displays, and sensors have been fabricated by combining conducting polymers. We report optical fibers and avalanche diodes as new functions of cyborg plants; the sprout/PANI composite has demonstrated avalanche diode functionality which is comparable to that of inorganic semiconductor devices that undergo "avalanche breakdown". Although the mechanism is different from that of inorganic semiconductors, this has led to the development of a new type of electrochemical diode.

Moreover, fucoidan/PANI composites are prepared by both the non-gel method and gel method via alkaline treatment in the polymerization process. The gel method for preparation of fucoidan/PANI can be called a double-step method. The water solution containing alkali improved the fluidity of the fucoidan, and aniline, as a monomer, was well

mixed in the solution. The addition of acid to the solution changed aniline to aniline salt with polymerization activity, and simultaneously, fucoidan, which was well-dissolved in the water, changed to the gel form. Polymerization of well-dispersed aniline in the fucoidan gel yielded fucoidan/PANI gel. Aniline monomer grew in the fucoidan gel as a chiral matrix to form PANI. The resultant PANI component is well dispersed in the fucoidan gel matrix to form the hybrid. The "gel-electrochemical polymerization" produced steady polymer films. Fucoidan can function as polymer gel reaction field that can produce high crystallinity in the resultant.

A summary of sprout/PANI and fucoidan/PANI, comparing the method of production and the properties of the resulting composites, is displayed in Table 3. Polymerization of the aniline was carried out with the bio-tissue (sprout) and biopolymer (fucoidan) in the form of non-gel and gel. The sprout/PANI has light conduction and avalanche diode function. The fucoidan/PANI exhibited a porous surface (power form) and electrochromism (film form).

Table 3. Summary of sprout/PANI and fucoidan/PANI.

Hybrid	Host	Polymerization	Function
sprout/PANI	Sprout (Bio-tissue)	Tissue surface (heterogeneous)	Optical conduction, avalanche breakdown
fucoidan/PANI	Fucoidan (Biopolymer)	(1) Non-gel method (heterogeneous) (2) Gel method (homogeneous)	Porous, electrochromism

PANI hybrids with biological tissue and bio-polymers can be synthesized for physiological-electroactive materials. Natural plants/conducting polymer materials are defined as plant cyborgs, and may be applied as fine electro-mechanically functional materials [50].

Author Contributions: H.G. carried out the preparation of the sprout/PANI hybrid and the IR analysis. M.I. performed synthesis of sprout/PANI and optical microscopy observations. H.G. carried out preparation of the sprout/PANI devices and M.I. measured the electrical function of the diode. M.O. carried out the electrochemical polymerization of sprout/PANI and measured the resultant film's properties. M.I. and H.G. wrote the main manuscript text, and H.G. prepared Tables 1–3, Schemes 1–3, and Figures 1–4, 11, 18–21 and 23. M.I. prepared Figures 5–10, 12 and 22. M.O. prepared Figures 12–17. All authors have read and agreed to the published version of the manuscript.

Funding: This work was supported by Japan Society for the Promotion of Science (JSPS), Grants-in-Aid for Scientific Research (No. 20K05626).

Institutional Review Board Statement: Not applicable.

Informed Consent Statement: Not applicable.

Data Availability Statement: Not applicable.

Acknowledgments: We would like to thank Kuniharu Nakajima (University of Tsukuba) for his contribution to the initial stages of this study.

Conflicts of Interest: The authors declare no conflict of interest.

References

1. Ito, T.; Shirakawa, H.; Ikeda, S. Simultaneous polymerization and formation of polyacetylene film on the surface of concentrated soluble Ziegler-type catalyst solution. *J. Polym. Sci. Polym. Chem.* **1974**, *12*, 11–20. [CrossRef]
2. Liu, X.; Liang, Y.; Yue, G.; Tu, Y.; Zheng, H. A dual function of high efficiency quasi-solid-state flexible dye-sensitized solar cell based on conductive polymer integrated into poly (acrylic acid-co-carbon nanotubes) gel electrolyte. *Sol. Energy* **2017**, *148*, 63–69. [CrossRef]
3. Chen, H.W.; Lee, J.H.; Lin, B.Y.; Chen, S.; Wu, S.T. Liquid crystal display and organic light-emitting diode display: Present status and future perspectives. *Light Sci. Appl.* **2018**, *7*, 17168. [CrossRef] [PubMed]
4. Guo, X.; Benavides-Guerrero, J.; Banerjee, D.; Roy-Moisan, F.; Cloutier, S.G. Hybrid color-tunable polymer light-emitting diodes using electrospraying. *ACS Omega* **2019**, *4*, 19287–19292. [CrossRef]

5. Jeon, S.O.; Lee, K.H.; Kim, J.S.; Ihn, S.G.; Chung, Y.S.; Kim, J.W.; Lee, H.; Kim, S.; Choi, H.; Lee, J.Y. High-efficiency, long-lifetime deep-blue organic light-emitting diodes. *Nat. Photonics* **2021**, *15*, 208–215. [CrossRef]
6. Iino, H.; Hanna, J. Liquid crystalline organic semiconductors for organic transistor applications. *Polym. J.* **2017**, *49*, 23–30. [CrossRef]
7. Lee, M.Y.; Lee, H.R.; Park, C.H.; Han, S.G.; Oh, J.H. Organic transistor-based chemical sensors for wearable bioelectronics. *Acc. Chem. Res.* **2018**, *51*, 2829–2838. [CrossRef]
8. Zhao, P.; Tang, Q.; Zhao, X.; Tong, Y.; Liu, Y. Highly stable and flexible transparent conductive polymer electrode patterns for large-scale organic transistors. *J. Colloid Interface Sci.* **2018**, *520*, 58–63. [CrossRef]
9. Abel, S.B.; Frontera, E.; Acevedo, D.; Barbero, C.A. Functionalization of conductive polymers through covalent postmodification. *Polymers* **2023**, *15*, 205. [CrossRef]
10. Bhadra, J.; Alkareem, A.; Al-Thani, N. A review of advances in the preparation and application of polyaniline based thermoset blends and composites. *J. Polym. Res.* **2020**, *27*, 122. [CrossRef]
11. Hu, Y.; Tong, X.; Zhuo, H.; Zhong, L.; Peng, X. Biomass-Based Porous N-Self-Doped Carbon Framework/Polyaniline Composite with Outstanding Supercapacitance. *ACS Sustain. Chem. Eng.* **2017**, *5*, 8663–8674. [CrossRef]
12. Jisha, P.; Suma, M.S.; Murugendrappa, M.V.; Raj, K. A study on the effect of PVDF on the structural and transport properties of polyaniline. *Int. J. Polym. Anal. Charact.* **2020**, *25*, 176–187. [CrossRef]
13. Kausar, A. Polyimide, polybenzimidazole-*in situ*-polyaniline nanoparticle and carbon nano-onion-based nanocomposite designed for corrosion protection. *Int. J. Polym. Anal. Charact.* **2017**, *22*, 557–567. [CrossRef]
14. Upadhyay, J.; Das, T.M.; Borah, R. Electrochemical performance study of polyaniline and polypyrrole based flexible electrodes. *Int. J. Polym. Anal. Charact.* **2021**, *26*, 354–363. [CrossRef]
15. Xu, H.; Zheng, D.; Liu, F.; Li, W.; Lin, J. Synthesis of an MXene/polyaniline composite with excellent electrochemical properties. *J. Mater. Chem. A* **2020**, *8*, 5853–5858. [CrossRef]
16. Zhang, Y.; Pan, T.; Yang, Z. Flexible polyethylene terephthalate/polyaniline composite paper with bending durability and effective electromagnetic shielding performance. *Chem. Eng. J.* **2020**, *389*, 124433. [CrossRef]
17. Demirci, S.; Sutekin, S.D.; Sahiner, N. Polymeric composites based on carboxymethyl cellulose cryogel and conductive polymers: Synthesis and characterization. *J. Compos. Sci.* **2020**, *4*, 33. [CrossRef]
18. Kausar, A. Potential of polymer/fullerene nanocomposites for anticorrosion applications in the biomedical field. *J. Compos. Sci.* **2022**, *6*, 394. [CrossRef]
19. Guo, Y.; Ghobeira, R.; Aliakbarshirazi, S.; Morent, R.; De Geyter, N. Polylactic acid/polyaniline nanofibers subjected to pre- and post-electrospinning plasma treatments for refined scaffold-based nerve tissue engineering applications. *Polymers* **2023**, *15*, 72. [CrossRef]
20. Komaba, K.; Goto, H. Preparation of bagworm silk/polyaniline composite. *J. Appl. Polym. Sci.* **2021**, *139*, e51791. [CrossRef]
21. Perrin, F.X.; Oueiny, C. Polyaniline thermoset blends and composites. *React. Funct. Polym.* **2017**, *114*, 86–103. [CrossRef]
22. Giraldo, J.P.; Landry, M.P.; Faltermeier, S.M.; McNicholas, T.P.; Iverson, N.M.; Boghossian, A.A.; Reuel, N.F.; Hilmer, A.J.; Sen, F.; Brew, J.A.; et al. Plant nanobionics approach to augment photosynthesis and biochemical sensing. *Nat. Mater.* **2014**, *13*, 400–408. [CrossRef] [PubMed]
23. Goto, H. Polymerisation of Aniline on the Butterfly Scale: Bio-Interface Polymerisation. *Int. Lett. Chem. Phys. Astron.* **2015**, *62*, 34–36. [CrossRef]
24. Komaba, K.; Goto, H. A polyaniline/shark skin composite and its conductivity based on polaron hopping. *Polym.-Plast. Technol. Mat.* **2020**, *60*, 906–916. [CrossRef]
25. Komaba, K.; Goto, H. Direct bio-interface preparation for spirulina and conductive polymer composite. *Int. J. Polym. Mater. Bio. Mater.* **2020**, *70*, 669–673. [CrossRef]
26. Komaba, K.; Hirokawa, S.; Goto, H. Preparation of biocarbon micro coils. *Soft Mater.* **2020**, *19*, 40–49. [CrossRef]
27. Sareen, H.; Maes, P. Cyborg botany: Exploring in-planta cybernetic systems for interaction. In *Extended Abstracts of the 2019 CHI Conference on Human Factors in Computing Systems*; ACM: New York, NY, USA, 2019; pp. 1–6. [CrossRef]
28. Stavrinidou, E.; Gabrielsson, R.; Gomez, E.; Crispin, X.; Nilsson, O.; Simon, D.T.; Berggren, M. Electronic plants. *Sci. Adv.* **2015**, *1*, e150113. [CrossRef]
29. Anisimov, Y.A.; Cree, D.E.; Wilson, L.D. Preparation of multicomponent biocomposites and characterization of their physico-chemical and mechanical properties. *J. Comp. Sci.* **2020**, *4*, 18. [CrossRef]
30. Gu, Z.J.; Song, W.; Shen, Q. Effect of electrostatic forces control on the structure and properties of polyaniline/graphene oxide nanocomposite. *Int. J. Polym. Anal. Charact.* **2019**, *24*, 517–523. [CrossRef]
31. Wang, L.; Yao, Q.; Xiao, J.; Zeng, K.; Qu, S.; Shi, W.; Wang, Q.; Chen, L. Engineered molecular chain ordering in single-walled carbon nanotubes/polyaniline composite films for high-performance organic thermoelectric materials. *Chem. Asian J.* **2016**, *11*, 1804–1810. [CrossRef]
32. Yamada, N. *Science of Sea Weed Fucoidan*; Seizando-Shoten Publishing Co., Ltd.: Tokyo, Japan, 2006; pp. 59, 79–85, 114–121, 151–161.
33. Usui, T.; Asari, K.; Mizuno, T. Isolation of highly purified "fucoidan" from *Eisenia bicyclis* and its anticoagulant and antitumor activities. *Agric. Biol. Chem.* **1980**, *44*, 1965–1966. [CrossRef]

34. Yamamoto, I.; Nagumo, T.; Yagi, K.; Tominaga, H.; Aoki, M. Antitumor effect of seaweeds. I. Antitumor effect of extracts from Sargassum and Laminaria. *Jpn. J. Exp. Med.* **1974**, *44*, 543–546.
35. Ponce, N.M.A.; Pujol, C.A.; Damonte, E.B.; Flores, M.L.; Stortz, C.A. Fucoidans from the brown seaweed *Adenocystis utricularis*: Extraction methods, antiviral activity and structural studies. *Carbohydr. Res.* **2003**, *338*, 153–165. [CrossRef]
36. De Jesus Raposo, M.F.; De Morais, A.M.B.; De Morais, R.M.S.C. Marine Polysaccharides from Algae with Potential Biomedical Applications. *Mar. Drugs* **2015**, *13*, 2967–3028. [CrossRef]
37. Willenborg, D.O.; Parish, C.R. Inhibition of allergic encephalomyelitis in rats by treatment with sulfated polysaccharides. *J. Immunol.* **1988**, *15*, 3401–3405. [CrossRef]
38. Filote, C.; Lanez, E.; Popa, V.I.; Lanez, T.; Volf, I. Characterization and Bioactivity of Polysaccharides Separated through a (Sequential) Biorefinery Process from *Fucus spiralis* Brown Macroalgae. *Polymers* **2022**, *14*, 4106. [CrossRef]
39. Kim, M.; Hayashi, M.; Yu, B.; Lee, T.K.; Kim, R.H.; Jo, D.-W. Effects of Fucoidan Powder Combined with Mineral Trioxide Aggregate as a Direct Pulp-Capping Material. *Polymers* **2022**, *14*, 2315. [CrossRef]
40. Hsiao, W.-C.; Hong, Y.-H.; Tsai, Y.-H.; Lee, Y.-C.; Patel, A.K.; Guo, H.-R.; Kuo, C.-H.; Huang, C.-Y. Extraction, Biochemical Characterization, and Health Effects of Native and Degraded Fucoidans from *Sargassum crispifolium*. *Polymers* **2022**, *14*, 1812. [CrossRef]
41. Akbari, A.; Bigham, A.; Rahimkhoei, V.; Sharifi, S.; Jabbari, E. Antiviral Polymers: A Review. *Polymers* **2022**, *14*, 1634. [CrossRef]
42. Arunagiri, V.; Tsai, H.-C.; Darge, H.F.; Hanurry, E.Y.; Lee, C.Y.; Lai, J.-Y.; Wu, S.-Y. Enhanced Cellular Uptake in an Electrostatically Interacting Fucoidan–L-Arginine Fiber Complex. *Polymers* **2021**, *13*, 1795. [CrossRef]
43. Apostolova, E.; Lukova, P.; Baldzhieva, A.; Katsarov, P.; Nikolova, M.; Iliev, I.; Peychev, L.; Trica, B.; Oancea, F.; Delattre, C.; et al. Immunomodulatory and Anti-Inflammatory Effects of Fucoidan: A Review. *Polymers* **2020**, *12*, 2338. [CrossRef] [PubMed]
44. Bernal-Ballen, A.; Lopez-Garcia, J.-A.; Ozaltin, K. (PVA/Chitosan/Fucoidan)-Ampicillin: A Bioartificial Polymeric Material with Combined Properties in Cell Regeneration and Potential Antibacterial Features. *Polymers* **2019**, *11*, 1325. [CrossRef] [PubMed]
45. Rohman, G.; Langueh, C.; Ramtani, S.; Lataillade, J.-J.; Lutomski, D.; Senni, K.; Changotade, S. The Use of Platelet-Rich Plasma to Promote Cell Recruitment into Low-Molecular-Weight Fucoidan-Functionalized Poly(Ester-Urea-Urethane) Scaffolds for Soft-Tissue Engineering. *Polymers* **2019**, *11*, 1016. [CrossRef] [PubMed]
46. Ozaltin, K.; Lehocky, M.; Humpolicek, P.; Pelkova, J.; Di Martino, A.; Karakurt, I.; Saha, P. Anticoagulant Polyethylene Terephthalate Surface by Plasma-Mediated Fucoidan Immobilization. *Polymers* **2019**, *11*, 750. [CrossRef]
47. Venkatesan, J.; Anil, S.; Kim, S.-K.; Shim, M.S. Seaweed Polysaccharide-Based Nanoparticles: Preparation and Applications for Drug Delivery. *Polymers* **2016**, *8*, 30. [CrossRef]
48. Belhadj, H.; Moulefera, I.; Sabantina, L.; Benyoucef, A. Effects of Incorporating Titanium Dioxide with Titanium Carbide on Hybrid Materials Reinforced with Polyaniline: Synthesis, Characterization, Electrochemical and Supercapacitive Properties. *Fibers* **2022**, *10*, 46. [CrossRef]
49. Perdigão, P.; Morais Faustino, B.M.; Faria, J.; Canejo, J.P.; Borges, J.P.; Ferreira, I.; Baptista, A.C. Conductive Electrospun Polyaniline/Polyvinylpyrrolidone Nanofibers: Electrical and Morphological Characterization of New Yarns for Electronic Textiles. *Fibers* **2020**, *8*, 24. [CrossRef]
50. Kudo, Y.; Goto, H. Bio-interface Polymerisation: Synthesis of Polyaniline on the Marine Algae Surface. *Int. Lett. Nat. Sci.* **2016**, *51*, 14–20. [CrossRef]

Disclaimer/Publisher's Note: The statements, opinions and data contained in all publications are solely those of the individual author(s) and contributor(s) and not of MDPI and/or the editor(s). MDPI and/or the editor(s) disclaim responsibility for any injury to people or property resulting from any ideas, methods, instructions or products referred to in the content.